Motion of a Brownian particle in the presence of reactive boundaries

Arnab Pal
School of Chemistry, Raymond and Beverly Sackler Faculty of Exact Sciences, Tel Aviv University, Tel Aviv 69978, Israel; Center for the Physics and Chemistry of Living Systems, Tel Aviv University, 6997801, Tel Aviv, Israel; and Sackler Center for Computational Molecular and Materials Science, Tel Aviv University, 6997801, Tel Aviv, Israel

Isaac Pérez Castillo
Departamento de Física Cuántica y Fotónica, Instituto de Física, Universidad Nacional Autónoma de México, Cd. de México C.P. 04510, México

Anupam Kundu
International Centre for Theoretical Sciences, TIFR, Bangalore 560089, India

(Received 19 April 2019; published 21 October 2019; corrected 12 October 2020)

We study the one-dimensional motion of a Brownian particle inside a confinement described by two reactive boundaries which can partially reflect or absorb the particle. Understanding the effects of such boundaries is important in physics, chemistry, and biology. We compute the probability density of the particle displacement exactly, from which we derive expressions for the survival probability and the mean absorption time as a function of the reactive coefficients. Furthermore, using the Feynman-Kac formalism, we investigate the local time profile, which is the fluctuating time spent by the particle at a given location, both till a fixed observation time and till the absorption time. Our analytical results are compared to numerical simulations, showing perfect agreement.

DOI: 10.1103/PhysRevE.100.042128

I. INTRODUCTION

Brownian motion is a paradigm of stochastic processes which has been studied quite extensively [1]. This simple process often successfully provides a basic description of various phenomena ranging from simple chemical reactions to complex biomolecular processes occurring at cellular and subcellular levels [2,3]. For instance, the motion of a protein molecule inside a living cell can be considered as a simple Brownian motion [2–4]. The protein molecules perform everlasting motions due to their thermal energy, and, as a result, the trajectory of the protein molecule is erratic and the density of the molecules slowly spreads throughout the medium. While diffusion can predict motion of protein molecules well inside the cellular domain under dilute conditions, the behavior gets affected by the nature of the boundaries [2–4]. This could be due to the structure of the cell membrane that protects and organizes cells by regulating not only what enters or exits the cell but also by how much [5,6]. Such gatekeeping functionalities of the boundaries (semipermeable or resistive in nature) are important to optimally control the flow of essential chemical species across the cellular membrane [7,8]. In this paper we address this issue in the context of noninteracting Brownian motion in the presence of reactive boundaries.

The simplest types of boundary conditions can be formulated in terms of either vanishing flux through the boundary (usually called reflecting or impermeable boundary) or vanishing density at the boundary (called the absorbing boundary) [9–21]. In the first case, a diffusing molecule is reflected whenever it hits the boundary, while in the second type of boundary condition a diffusing molecule is removed from the system whenever it hits the boundary, which can be interpreted as the molecule being absorbed at the boundary. However, more realistic boundary conditions can be realized in terms of a partially absorbing boundary (also termed Robin, radiative, or mixed boundary conditions [3]), which means that a molecule may be absorbed (or reflected) with some probability [22–31]. From a biochemical point of view, this absorption probability depends on the reactivity of the boundary (e.g., on the rate constant of the adsorbing chemical reaction and on the number of available receptors) and on the details of the model. The reactivity constant can also be measured experimentally from the chemical properties of the boundary (see, e.g., Ref. [8] and references therein).

The interaction of a diffusive particle with a reactive boundary is also of practical importance, since they offer plentiful industrial applications in surface or colloid science and materials research [32]. A few examples worth mentioning are fluid or mass transport in porous media [33], electric transport in electrolytic cells [34], nuclear magnetic resonance (diffusion of spins in confining porous media), and applications to foam relaxation and surfactants [35]. Other examples can be found in physiology where oxygen molecules can penetrate across alveolar membranes for further adsorption in blood or are bounced back and continue the motion. The proportion of adsorbed and reflected oxygen molecules can be characterized by permeability varying from zero (perfectly reflecting boundary) to infinity (perfectly adsorbing boundary) [36–38]. A similar description can be useful to explain heterogeneous catalysis frequently observed in petrochemistry, e.g., chemical

vapor decomposition or plasma etching [20]. The reactive molecules are injected into a solvent, and then they diffuse towards a catalyst. Hitting the catalytic surface, they can be either transformed into other molecules (with a finite reaction rate) or are bounced back for further diffusion in the bulk [39–41].

In this paper we investigate the motion of noninteracting diffusing molecules inside a reactive domain. If left alone the molecules may eventually get adsorbed at the boundary of the confining domain after some time. This is called the lifetime when the molecule gets adsorbed. Clearly, this time is a random quantity whose cumulative probability, called the survival probability, simply measures the chance for the species to remain inside a confining domain up to a fixed time t without being absorbed. In the literature, computing this distribution is known as the first passage time problem, and it has been a subject of interest to scientists for many decades [42–46]. First passage time problems have ubiquitous applications in physical, biological, and chemical processes, ranging from finance to animal foraging theory. More concretely, some examples are survival time of a bacteria to remain alive while searching for food, average lifetime of a messenger RNA which is translated into protein by the joint action of transfer RNA (tRNA) and the ribosome, binding time of a protein to an enzyme, and search time of animals for food resources, to name just a few. [42–46]. Motivated by this backdrop, we investigate the survival properties of diffusive particles inside a reactive domain [47,48]. In addition, we are also interested in the extreme displacements made by the diffusing particle and time spent per unit length around a spatial point in the presence of reactive boundaries. This time density is usually referred to as the local time density or the reaction time. These quantities are important in characterizing the motion of the molecule. Indeed, the extreme displacement describes the geometrical properties of the trajectories of the molecule, while the local time captures the temporal distribution of the trajectories over space and, as such, provides the time spent by a molecule near a reactive agent placed at a specific region of the space, upon which the reaction takes place.

In the present paper, we have organized our results into three parts. In Sec. II we obtain exact analytical results for the propagator, survival probability, and mean adsorption time. In Sec. III we compute the distribution of the maximum displacement of the molecule by the method of counting paths. In Sec. IV we study the statistical properties of the local time using the Feynman-Kac method of Brownian functionals in two cases: (1) when the observation time is fixed and (2) when the observation time is random. In all cases, we have verified our results by contrasting them to numerical simulations, which are explained in Sec. V. The conclusions and outlooks of our work are presented in Sec. VI. Finally, for sake of clarity, some of the derivations have been detailed to the appendices.

II. PROPAGATOR, SURVIVAL PROBABILITY, AND ABSORPTION PROBABILITY

We consider a Brownian molecule moving in one dimension inside a domain $x \in [0, L]$ with partially absorbing boundaries. The motion of the molecule is described by a propagator $G_L(x, x_0, t)$, which simply represents the probability density for the molecule to be found at x at time t given that it started at x_0 at an initial time $t_0 = 0$. It can be shown that the propagator satisfies the diffusion equation subject to the reactive boundary conditions at $x = 0$ and $x = L$:

$$\frac{\partial}{\partial t} G_L(x, x_0, t) = D \frac{\partial^2}{\partial x^2} G_L(x, x_0, t), \tag{1}$$

$$\frac{\partial}{\partial x} G_L(0, x_0, t) = \alpha_0 G_L(0, x_0, t), \tag{2}$$

$$\frac{\partial}{\partial x} G_L(L, x_0, t) = -\alpha_L G_L(L, x_0, t), \tag{3}$$

where D is the diffusion constant. For clarity, we will consider deterministic initial conditions: $G_L(x, x_0, 0) = \delta(x - x_0)$. The parameter $\alpha_0 \geqslant 0$ (resp. $\alpha_L \geqslant 0$), often known as the reactive constant, controls how often a molecule hitting the boundary at $x = 0$ (resp. $x = L$) will be either reflected or absorbed. This can be easily seen from Eq. (2). For $\alpha_0 = 0$ Eq. (2) becomes $(\partial G_L/\partial x)_{x=0} = 0$, which is the boundary condition for a reflective wall. On the other hand, if $\alpha_0 \to \infty$ then one gets $G_L(x = 0, x_0, t) = 0$ from Eq. (2), which is the boundary condition for an absorbing wall. Thus by tuning these values one can go from a perfectly reflecting boundary ($\alpha_0 = 0$) to a perfectly absorbing boundary ($\alpha_L = \infty$). For a finite value of α_0 the particle, upon hitting the wall, may not always get absorbed. The probability for which it gets absorbed (or reflected) depends on α_0 [see Eq. (56) in Sec. V]. A similar interpretation holds also for Eq. (3). Further details on this physical interpretation can be found in Ref. [12].

The problem of finding the propagator has been considered earlier in several contexts, for example, with a step initial condition for the concentration [49], in target search problems [50], or in diffusion-controlled recombinations [51]. It has been shown that solving the diffusion equation in a bounded domain with reactive boundary conditions is equivalent to solving the diffusion equation in an unbounded domain with "sink" terms [44,49].

For convenience and completeness we here rederive the propagator by solving Eq. (1) inside the domain $x \in [0, L]$ satisfying the reactive boundary conditions (2) and (3) and the deterministic initial condition $G_L(x, x_0, t = 0) = \delta(x - x_0)$. Applying the method of separation of variables in Eq. (1), it is easy to show that one can write the propagator in the following form [52]:

$$G_L(x, x_0, t) = \sum_{k \in \mathcal{R}_k(L)} e^{-Dk^2 t} \frac{k \cos(kx) + \alpha_0 \sin(kx)}{\alpha_0^2 + k^2} \times \frac{k \cos(kx_0) + \alpha_0 \sin(kx_0)}{L + \frac{\alpha_0}{\alpha_0^2 + k^2} + \frac{\alpha_L}{\alpha_L^2 + k^2}}. \tag{4}$$

Here $\mathcal{R}_k(L)$ is the set of eigenvalues obtained by solving the following transcendental equation for a fixed value of L [52]:

$$e^{2ikL} = \frac{(k + i\alpha_0)(k + i\alpha_L)}{(k - i\alpha_0)(k - i\alpha_L)}. \tag{5}$$

Various limits can be immediately examined from Eq. (4). For example, in the case of a semi-infinite domain (where the boundary at $x = L$ is taken to infinity) the propagator takes the

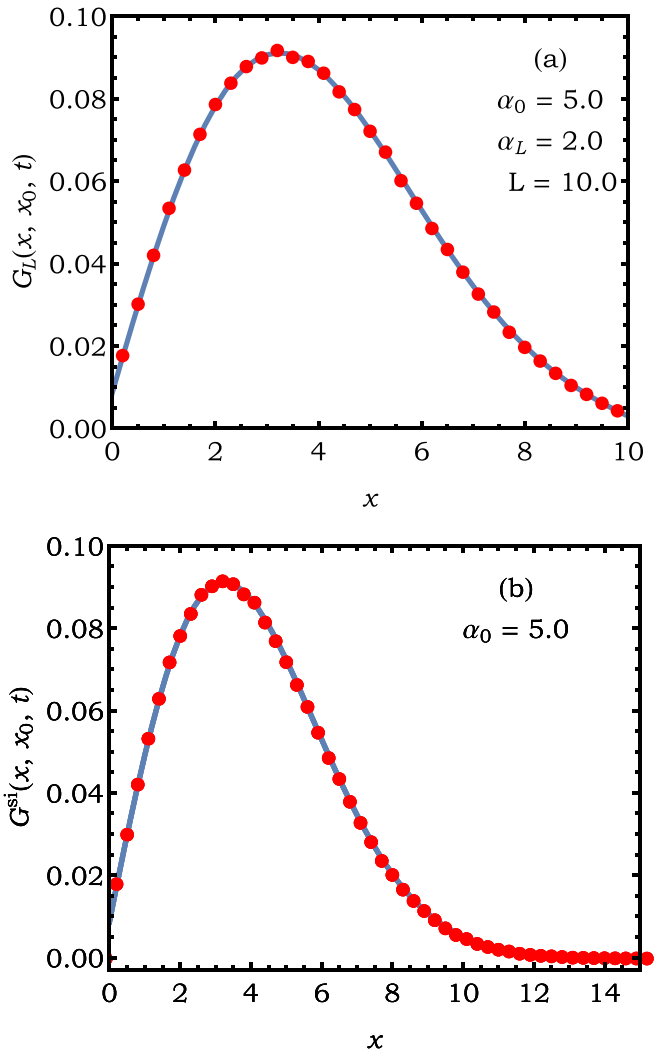

FIG. 1. Probability distribution of a Brownian molecule inside the interval $[0, L]$ with reactive boundaries at $x = 0$ and $x = L$ till an observation time $t = 5$. (a) The comparison between the theory given by Eq. (4) (solid blue line) and Monte Carlo simulations (red circles) for the probability distribution of the molecule displacement when it diffuses strictly inside the box. (b) Similarly, the semi-infinite domain obtained by taking the boundary at L to be at infinity and comparing the results for the probability distribution of its displacement between Monte Carlo simulations (red circles) and the exact formula (solid blue line) given by Eq. (6).

following form (see Appendix A for details):

$$G^{\rm si}(x, x_0, t) = \frac{1}{4\alpha_0} e^{D\alpha_0^2 t} \mathcal{D}_x \mathcal{D}_{x_0} \times [\phi(x - x_0, t) - \phi(x + x_0, t)], \quad (6)$$

where $\mathcal{D}_y = (\frac{\partial}{\partial y} + \alpha_0)$, and the function ϕ is defined as

$$\phi(z, t) = e^{\alpha_0 z} \mathrm{erfc}\left[\frac{2D\alpha_0 t + z}{\sqrt{4Dt}}\right] + e^{-\alpha_0 z} \mathrm{erfc}\left[\frac{2D\alpha_0 t - z}{\sqrt{4Dt}}\right]. \quad (7)$$

In Fig. 1 we have compared our analytical results to Monte Carlo simulations, which were performed according to the method explained in Sec. V. The top panel corresponds to taking a finite-size interval, while the bottom panel is the result of considering a semi-infinite domain. In both cases the agreement between theory and Monte Carlo simulations is excellent.

Due to the presence of the reactive boundaries, the probability current leaks out through them, and, as a result, the survival probability that a molecule has not been absorbed till the observation time t decreases with time. This probability can be obtained from the propagator $G_L(x, x_0, t)$ as

$$S_L(x_0, t) = \int_0^L dx G_L(x, x_0, t). \quad (8)$$

A simple interpretation of Eq. (8) comes from a path-counting argument and works as follows. The propagator contains the contributions from all the statistical paths that start at time $t_0 = 0$ at position x_0 and end at time t at position x without being absorbed at either boundaries. There are four types of such paths: those which have never reached either boundaries at $x = 0$ and $x = L$ in time t, those which may have hit one of the boundaries but got reflected, and those which may have hit both boundaries and, again, got reflected. The survival probability then gets a contribution from all such paths which reach any final point $x \in (0, L)$. Integrating the final position x from 0 to L in the expression of the propagator $G_L(x, x_0, t)$, we get

$$S_L(x_0, t) = \sum_{k \in \mathcal{R}_k(L)} e^{-Dk^2 t} \frac{\alpha_0[1 - \cos(kL)] + k \sin(kL)}{k(\alpha_0^2 + k^2)} \times \frac{k \cos(kx_0) + \alpha_0 \sin(kx_0)}{L + \frac{\alpha_0}{\alpha_0^2 + k^2} + \frac{\alpha_L}{\alpha_L^2 + k^2}}. \quad (9)$$

In the limit of $L \to \infty$, the survival probability at the boundary 0 till an observation time t can be obtained either from Eq. (9) or by integrating out the final position x in $G^{\rm si}(x, x_0, t)$ from zero to infinity. Either way, the final result is

$$S(x_0, t) = e^{D\alpha_0^2 t + \alpha_0 x_0} \mathrm{erfc}\left[\frac{x_0 + 2D\alpha_0 t}{\sqrt{4Dt}}\right] + \mathrm{erf}\left[\frac{x_0}{\sqrt{4Dt}}\right], \quad (10)$$

which, as shown in Fig. 2, agrees with estimates obtained by Monte Carlo simulations. It is easy to verify from Eq. (10) that when the boundary is completely reflective ($\alpha_0 \to 0$) the process always survives, that is, $S(x_0, t) = 1$. On the other hand, for a completely absorbing boundary condition ($\alpha_0 \to \infty$) we readily recover the well-known result $S(x_0, t) = \mathrm{erf}[x_0/\sqrt{4Dt}]$ [44]. Note also that at large time, $S(x_0, t) \sim 1/\sqrt{t}$ as expected and shown in the inset of Fig. 2.

Next, we focus on the time at which the particle gets absorbed at the boundaries. Clearly this time is a stochastic quantity, similar to the concept of the first passage time [42–46], and we are interested in its statistical properties. In our case, however, as the particle may not get absorbed when it hits the boundary for the first time due to the mixed boundary conditions, we look instead at the time t_a when the particle

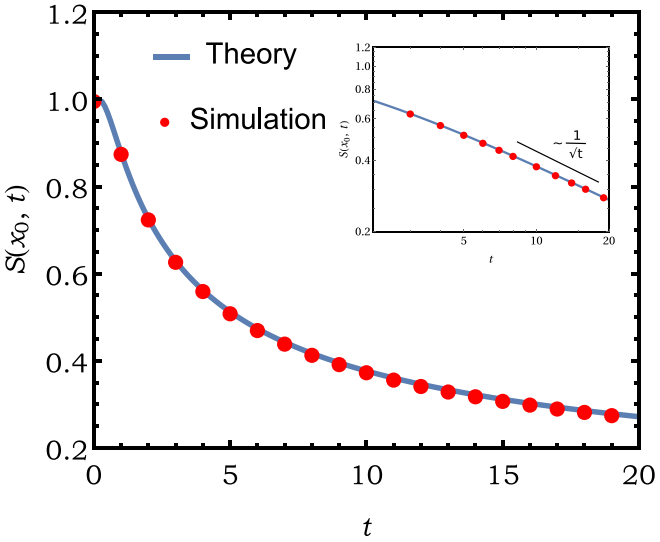

FIG. 2. Comparison of the expression Eq. (10) of the survival on the semi-infinite line with a reactive boundary at the origin with an estimate obtained from numerical simulations. We have used the following parameters for the simulation: $\alpha_0 = 5$, $D = 1$, and $x_0 = 2$. The simulation data (red circles) is in excellent agreement with the analytical result (solid blue line). Inset: The survival probability in the log-log scale, which shows an excellent match with $1/\sqrt{t}$ behavior in the large time as predicted from the theoretical analysis.

gets absorbed at either boundary. Its probability density function, denoted by $f_L(x_0, t)$, is related to the survival probability as $f_L(x_0, t) = -\frac{dS_L(x_0,t)}{dt}$, which immediately implies that the mean absorption time is given by

$$T_L(x_0) = \int_0^\infty dt\, t f_L(x_0, t) = \int_0^\infty dt S_L(x_0, t). \tag{11}$$

Using the explicit form of $S_L(x_0, t)$ in Eq. (9) in the above equation we get

$$T_L(x_0) = \sum_{k\in\mathcal{R}_k(L)} \frac{\alpha_0[1-\cos(kL)] + k\sin(kL)}{Dk^3(\alpha_0^2+k^2)} \times \frac{k\cos(kx_0) + \alpha_0\sin(kx_0)}{L + \frac{\alpha_0}{\alpha_0^2+k^2} + \frac{\alpha_L}{\alpha_L^2+k^2}}. \tag{12}$$

In the presence of two completely absorbing boundaries at 0 and at L (that is, by taking the limits $\alpha_0 \to \infty$ and $\alpha_L \to \infty$), the expression of the mean absorption time becomes simpler:

$$T_L^{\rm abs}(x_0) = \frac{2L^2}{D\pi^3}\sum_{n=1}^{\infty}\frac{1-(-1)^n}{n^3}\sin\left(\frac{n\pi x_0}{L}\right) = \frac{L^2}{2D}z(1-z), \tag{13}$$

where $z = x_0/L$, and we recover this previously obtained result [44,53]. On the other hand, by taking the semi-infinite limit ($L \to \infty$) with finite α_0, the mean absorption time diverges, as expected [44].

III. DISTRIBUTION OF MAXIMUM DISPLACEMENT

Inside a cellular domain, protein molecules perform short excursions before they either react to substrates or get absorbed at the boundaries. The nature of these paths depends on several factors such as cell concentration or local density of the surrounding molecules. In this biological scenario, very long trajectories may be detrimental for chemical reactions at the boundaries to occur but can be useful when a longer lifetime of a molecule (i.e., with small absorption probability at the boundaries) is favored. Moreover, often the amount of space visited by a diffusing chemical reagent inside a cell becomes quite important as it might control the yield of a reaction. One of the simplest measures of such excursions in one dimension is the maximum displacement realized by the molecule.

A. Maximum displacement till a fixed time t

Let M be the maximum displacement made by the molecule till time t. The cumulative probability that M is less than L, denoted by $H(L, t|x_0) = \text{Prob}[M \leqslant L, t|x_0]$, can be expressed as the following ratio:

$$H(L, t|x_0) = \frac{\mathcal{S}_L(x_0, t)}{\mathcal{S}_\infty(x_0, t)}, \tag{14}$$

where $\mathcal{S}_L(x_0, t) = \int_0^L \mathcal{G}_L(x, x_0, t)$ is the survival probability of the molecule in the presence of a completely absorbing boundary at L in addition to a reactive boundary at $x = 0$. Here $\mathcal{G}_L(x, x_0, t)$ is the propagator which describes such a system. Therefore, $\mathcal{G}_L(x, x_0, t) = \lim_{\alpha_L\to\infty} G_L(x, x_0, t)$ and consequently $\mathcal{S}_\infty(x_0, t) = \lim_{L\to\infty} \mathcal{S}_L(x_0, t)$. Again the expression in Eq. (14) can be understood from a very simple path-counting argument. The cumulative probability $H(L, t|x_0)$ gets a contribution from all the paths which start from x_0 and reach somewhere within $x \in (0, L)$ (while staying below $x = L$ throughout) along with the condition that they survived the reactive boundary at $x = 0$ till time t. Hence this probability is exactly the fraction of paths of duration t that starting from x_0 never hit $x = L$ among those paths which survive till time t from the reactive boundary at $x = 0$.

Taking the $\alpha_L \to \infty$ limit in Eq. (4), we get the corresponding propagator inside a box $0 \leqslant x \leqslant L$ of size L with an completely absorbing boundary at $x = L$ and a partially reflecting boundary at $x = 0$:

$$\mathcal{G}_L(x, x_0, t) = \lim_{\alpha_L\to\infty} G_L(x, x_0, t) = \sum_k e^{-Dk^2t}\frac{[k\cos(kx) + \alpha_0\sin(kx)]}{L(\alpha_0^2+k^2) + \alpha_0} \times [k\cos(kx_0) + \alpha_0\sin(kx_0)], \tag{15}$$

with

$$e^{2ikL} = -\frac{(k+i\alpha_0)}{(k-i\alpha_0)}. \tag{16}$$

Integrating the final position x of this propagator from 0 to L, we get the associated survival probability $\mathcal{S}_L(x_0, t)$ of the particle:

$$\mathcal{S}_L(x_0, t) = \int_0^L dx\, \mathcal{G}_L(x, x_0, t). \tag{17}$$

Once we know $\mathcal{S}_L(x_0,t)$, we can use Eq. (14) to obtain an expression for $H(L,t|x_0)$. Clearly, in the limits $L\to\infty$ and $t\to\infty$, while keeping $\ell=\frac{L}{\sqrt{Dt}}$ constant, the survival probability $\mathcal{S}_L(x_0,t)$ can be written in terms of the scaled variable $z_0=\frac{x_0}{\sqrt{Dt}}$ such that $\mathcal{S}_L(x_0,t)=s_\ell(z_0,t)$. After performing some algebraic manipulations one finds

$$s_\ell(z_0,t)\simeq 2\alpha_0\sqrt{Dt}\;\ell^2\sum_{n=1}^{\infty}\frac{[1-(-1)^n]\left[\frac{n\pi}{\ell}\cos\left(\frac{n\pi z_0}{\ell}\right)+\sqrt{Dt}\alpha_0\sin\left(\frac{n\pi z_0}{\ell}\right)\right]}{n\pi\left[n^2\pi^2+Dt\;\alpha_0^2\;\ell^2+\sqrt{Dt}\;\alpha_0\;\ell\right]}\;e^{-\frac{n^2\pi^2}{\ell^2}}. \tag{18}$$

To arrive at the above expression we have replaced $kL=p\ell$ in Eq. (15) to obtain the transcendental equation

$$\frac{p}{\tan(p\ell)}=-\alpha_0\sqrt{Dt}. \tag{19}$$

For large t, the solution of this equation is given approximately by $p\approx\frac{n\pi}{\ell}$ with $n=1,2,3,\ldots$. Hence by taking a derivative in Eq. (14), we obtain the following scaling form for the distribution $P_{x_0}(M,t)$ of the maximum:

$$P_{x_0}(M,t)=\frac{1}{\sqrt{Dt}}\;f_{x_0/\sqrt{Dt}}\left(\frac{M}{\sqrt{Dt}},t\right), \tag{20}$$

where

$$f_{z_0}(m,t)=\frac{1}{\lim\limits_{\ell\to\infty}s_\ell(z_0,t)}\left[\frac{\partial s_\ell(z_0,t)}{\partial\ell}\right]_{\ell=m} \tag{21}$$

is the scaling function with the scaled maximum displacement $m=M/\sqrt{Dt}$. In Fig. 3(a) we have compared the expression of $\sqrt{Dt}P_{x_0}(M,t)$, given by Eq. (20), with the corresponding estimate obtained by Monte Carlo simulations. As can be appreciated in Eq. (20), when plotted in this way we observe nice agreement with the numerical data (disks) with the theoretical curve (solid line) from Eq. (21) for $x_0=2$, $D=1$, and $t=100$. Note that the solutions $p=n\pi/\ell$, $n=1,2,\ldots$ of the transcendental equation in (19) are valid for $\ell\lesssim O(1)$ with $\sqrt{Dt}\gg\alpha_0^{-1}$. Hence the "scaling" form of the distribution of the maximum given in terms of the scaling variable $\ell=M/\sqrt{Dt}$ in Eqs. (20) and (21) is valid at times $t\gg(D\alpha_0)^{-2}$ for $M\lesssim\sqrt{Dt}$. Following a similar procedure it can be shown that for fixed t the distribution $P_{x_0}(M,t)$ decays at the right tail ($M\to\infty$) as $\sim 1/M^2$.

For a completely absorbing boundary at $x=0(\alpha_0\to\infty)$, the root equation in Eq. (15) becomes $\tan(p\ell)=0$. This gives us the solutions $p=\frac{n\pi}{\ell}$ for $n=1,2,3,\ldots$, from which we derive the following form of the scaled survival probability:

$$s_\ell(z_0,t)=\frac{2}{\pi}\sum_{n=1}^{\infty}\frac{1-(-1)^n}{n}\;\sin\left(\frac{n\pi z_0}{\ell}\right)e^{-\frac{n^2\pi^2}{\ell^2}}, \tag{22}$$

which matches with previously derived results [53].

B. Distribution of maximum displacement till the first absorption time

It is also important to know up to what extent the molecule has explored a region before it got absorbed at the reactive boundary. This can be quantified by the maximum displacement M made by the molecule till the absorption time. The cumulative distribution $Q_a(L|x_0)=\text{Prob.}[M\leqslant L|x_0]$ of this maximum M can be obtained from

$$Q_a(L|x_0)=D\int_0^\infty dt\left(\frac{\partial\mathcal{G}_L}{\partial x}\right)_{x=0}, \tag{23}$$

which can be understood by looking at the exit problem for the particle from the box $x\in[0,L]$ with a partially absorbing boundary at $x=0$ (α_0 finite) and a perfectly absorbing boundary at $x=L$ ($\alpha_L\to\infty$). Note that this perfectly absorbing boundary makes sure that the maximum displacement M till some time t is less than L, of course, conditioned on survival. Since we want the distribution of the maximum till the absorption at the partially absorbing wall at $x=0$, we should look only at those trajectories in which the particle starting from x_0 never touches the right boundary at $x=L$ till it gets absorbed at (or exits the box through) the boundary at $x=0$. Hence, we have $Q_a(L|x_0)=\frac{F_a(L|x_0)}{H_a(x_0)}$, where $F_a(L|x_0)$ is the probability that the particle escapes through the left boundary at 0 and $H_a(x_0)=\lim\limits_{L\to\infty}F_a(L|x_0)$. Even in the $L\to\infty$ limit, the particle will eventually get absorbed at $x=0$ in one dimension, which means in $H_a(x_0)=1$. This simply gives $Q_a(L|x_0)=F_a(L|x_0)$. On the other hand, by definition we have

$$F_a(L|x_0)=\int_0^\infty dt\;f_a(t|x_0,L), \tag{24}$$

where $f_a(t|x_0,L)$ is the first passage time density, which accounts for the probability that the particle gets absorbed at $x=0$ at time t without hitting the other boundary at L. This time density $f_a(t|x_0,L)$ represents the contribution to the decay of the survival probability $\mathcal{S}_L(t)$ of the particle coming from the (probability) current leakage through the boundary at $x=0$. The rate at which this leakage happens is given by $f_a(t|x_0,L)=D\frac{\partial\mathcal{G}_L}{\partial x}|_{x=0}$ [44] where $\mathcal{G}_L$ [see Eq. (15)] represents the propagator of the particle moving inside this box. Substituting this relation in Eq. (24), we arrive at Eq. (23). After using the explicit expression of $\mathcal{G}_L$ from Eq. (15) and performing some manipulations we get

$$Q_a(L|x_0)=\alpha_0\sum_k\frac{[k\cos(kx_0)+\alpha_0\sin(kx_0)]}{k\left[\alpha_0+L\left(\alpha_0^2+k^2\right)\right]}, \tag{25}$$

with

$$e^{2ikL}=\frac{(k+i\alpha_0)}{(k-i\alpha_0)}. \tag{26}$$

Hence, the distribution of the maximum $P_a(M,x_0)$ till absorption time is obtained from

$$P_{f_a}(M,x_0)=\left[\frac{\partial Q_a(L|x_0)}{\partial L}\right]_{L=M} \tag{27}$$

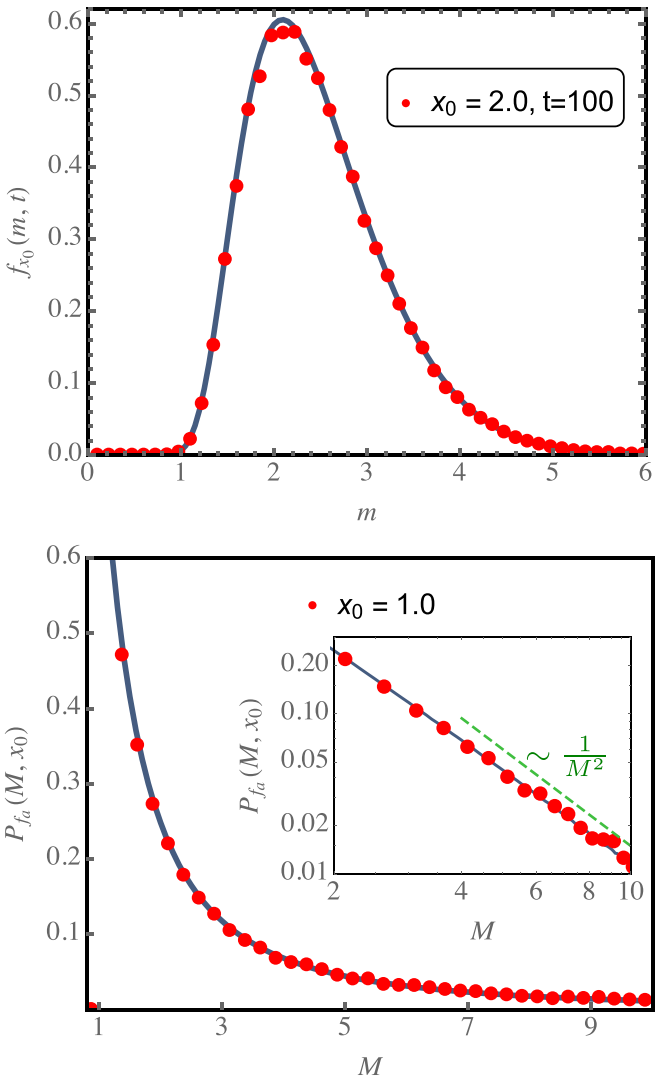

FIG. 3. (a) The probability distribution $f_{z_0}(m,t)$ function given in Eq. (21) of the scaled maximum displacement m. The red disks are the results from Monte Carlo simulations for $x_0 = 2$, $t = 100$ with $\alpha_0 = 5$ and $D = 1$. The solid line represents the theoretical curve given by Eq. (20). An excellent agreement between the theoretical curve and numerical data is observed. (b) The probability distribution of the maximum excursion $P_{f_a}(M,x_0)$ performed by the molecule before it is absorbed by the reactive boundary at the origin. The red disks are obtained from simulations and plotted along with the theoretical result (solid line) in Eq. (27). Inset: The large M asymptotic as $\sim\frac{1}{M^2}$ (dashed line) in the log-log scale along with its numerical verification (disks). The parameters for panel (b) are $D = 1$, $\alpha_0 = 5$, observation time $t = 100$, and $x_0 = 1$.

We have plotted Eq. (27) against numerical simulations in Fig. 3(b), and we observe an excellent agreement between them. In this case, it is also easy to show from Eqs. (25)–(27) that, for large M, the distribution of the maximum decays as $\sim 1/M^2$. To show this we use the fact that at large L the solutions of the Eq. (26) are given by $k \approx \frac{(2n+1)\pi}{L}$ with $n = 0, 1, 2, \ldots$. Substituting these solutions in Eq. (25) and converting the sum to integrals for large L one finds $Q_a(L|x_0) = C_1 - \frac{C_2}{L}$, where $C_{1,2}$ are constants depending on D, x_0 and α_0. Taking the derivative with respect to L that appears in Eq. (27), we immediately see $P_{f_a}(M,x_0) \sim C_2/M^2$. This power-law tail is verified numerically in the inset of Fig. 3(b).

As done previously, in the case of maximum distribution till absorption as well, it is important to check the various limits which have been studied earlier. For example, in the case when the boundary at $x = 0$ becomes fully absorbing ($\alpha_0 \to \infty$), one can show that the scaled cumulative distribution is given by

$$Q_a(z_0,\ell) = 2\sum_{n=1}^{\infty} \frac{\sin\left(\frac{n\pi x_0}{L}\right)}{n\pi} = 1 - \frac{x_0}{L}, \tag{28}$$

which reproduces the result derived in Ref. [53].

IV. LOCAL TIME SPENT AT y_0 TILL A FIXED TIME t

In this section we look at the local time density $L_t(y_0,x_0)$, defined as

$$L_t(y_0,x_0) = \int_0^t dt' \delta[x(t') - y_0|x_0], \tag{29}$$

which measures the amount of time the Brownian molecule spends at a given coordinate y_0 over an interval $0 \leqslant t' \leqslant t$, given that it had started from x_0. By construction, this is a functional of the trajectory and normalized as $\int dy_0\ L_t(y_0,x_0) = t$. This quantity is important in various situations. For example, in the kinetics of an enzymatic reaction mechanism, an enzyme binds to a substrate to form a complex, which in turn releases a product, regenerating the original enzyme. The reaction or binding time of such process is very relevant in biochemistry since prior knowledge could help improve the efficiency of a chemical reaction through catalysis or by facilitating metabolic pathways.

Statistical properties of L_t has been studied in the context of Brownian motion in bounded geometry with either completely absorbing or reflecting boundaries [43,54–58]. In the context of a generic Markov process the local time density is known as the empirical density (when appropriately rescaled by the observation time) [59,60]. In this section we study the local time density in presence of partially absorbing boundaries.

In order to compute the statistical properties of L_t, we introduce the generating function

$$\mathcal{Q}_p(y_0,x_0,t) = \langle e^{-pL_t(y_0,x_0)}\rangle, \tag{30}$$

where the average is performed with respect to the probability density $P(L_t|x_0,y_0,t)$ of the local time. This average can be written explicitly after taking into account the exact path measure

$$\mathcal{Q}_p(y_0,x_0,t) = \frac{1}{S_L(x_0,t)}\int_0^L dx \int_{x(0)=x_0}^{x(t)=x} \mathcal{D}[x(\tau)] \times e^{-\int_0^t d\tau\{\frac{1}{4D}[\frac{dx(\tau)}{d\tau}]^2 + p\delta(x(\tau)-y_0)\}}, \tag{31}$$

where the survival probability $S_L(x_0,t)$ weighs the surviving paths [see Eq. (9)]. Following the Feynman-Kac method and after introducing an appropriate Hamiltonian H_p, one can map the original problem of evaluating the above path integral into

the computation of an imaginary time quantum propagator:

$$\mathcal{Q}_p(y_0, x_0, t) = \frac{Q_p(y_0, x_0, t)}{S_L(x_0, t)}, \tag{32}$$

where

$$Q_p(y_0, x_0, t) = \int_0^L dx \langle x|e^{-t\hat{H}_p}|x_0\rangle, \tag{33}$$

with $\hat{H}_p(y_0) = -D\frac{d^2}{dx^2} + p\ \ \delta(x - y_0)$, and $S_L(x_0, t) = \int_0^L dx\ \langle x|e^{-t\hat{H}_0}|x_0\rangle$. Using the backward Kolmogorov approach, one can show that $Q_p(y_0, x_0, t)$ obeys the following Fokker-Planck equation:

$$\frac{\partial Q_p}{\partial t} = D\frac{\partial^2 Q_p}{\partial x_0^2} - p\delta(x_0 - y_0)Q_p, \tag{34}$$

with $Q_p(y_0, x_0, 0) = 1$, and boundary conditions

$$\left[\frac{\partial Q_p}{\partial x_0} - \alpha_0 Q_p\right]_{x_0=0} = 0,$$
$$\left[\frac{\partial Q_p}{\partial x_0} + \alpha_L Q_p\right]_{x_0=L} = 0. \tag{35}$$

The usual trick is then to write Eq. (34) in Laplace space with $\tilde{Q}_p(y_0, x_0, s) = \int_0^\infty dt\ e^{-st} Q_p(y_0, x_0, t)$ such that

$$D\frac{d^2\tilde{Q}_p}{dx_0^2} - [s + p\delta(x_0 - y_0)]\tilde{Q}_p = -1. \tag{36}$$

The boundary conditions given by Eq. (35) are automatically translated into

$$\left[\frac{\partial \tilde{Q}_p}{\partial x_0} - \alpha_0 \tilde{Q}_p\right]_{x_0=0} = 0,$$
$$\left[\frac{\partial \tilde{Q}_p}{\partial x_0} + \alpha_L \tilde{Q}_p\right]_{x_0=L} = 0. \tag{37}$$

In general, although it is possible to solve Eq. (36) with the corresponding boundary conditions (37), performing the inverse Laplace transform is, more often than not, rather cumbersome. We can nevertheless obtain some results in the large time limit for some special choices of the reactive constants α_0, α_L and the position y_0 where the local time is measured. In Appendix B we provide details of the computation of the first and second moments. In Fig. 4 we plot the mean local time $\langle L_t(y_0, t)\rangle$ and the variance $\langle L_t(y_0)^2\rangle - \langle L_t(y_0)\rangle^2$ as a function of time t measured at $y_0 = 0$ for $\alpha_L = 0$, $\alpha_0 = 2.0$, and $L = 2$. We notice that both these quantities grow linearly with time at large times (see Appendix B for further details) and observe nice agreement with the Monte Carlo simulations.

While only a few moments can be computed exactly in certain limits in the case of the finite box, it is, however, possible to push further the analytical results in the case of the semi-infinite domain. In this case we compute the distribution $P(L_t|x_0, y_0, t)$ of the local time density at $y_0 = 0$ and $y_0 = x_0$.

Let us start with the case $y_0 = 0$. Here the boundary conditions become rather simple,

$$\left[\frac{\partial \tilde{Q}_p}{\partial x_0} - \alpha_0 \tilde{Q}_p\right]_{x_0=0} = 0, \qquad \tilde{Q}_p|_{x_0\to\infty} = 1, \tag{38}$$

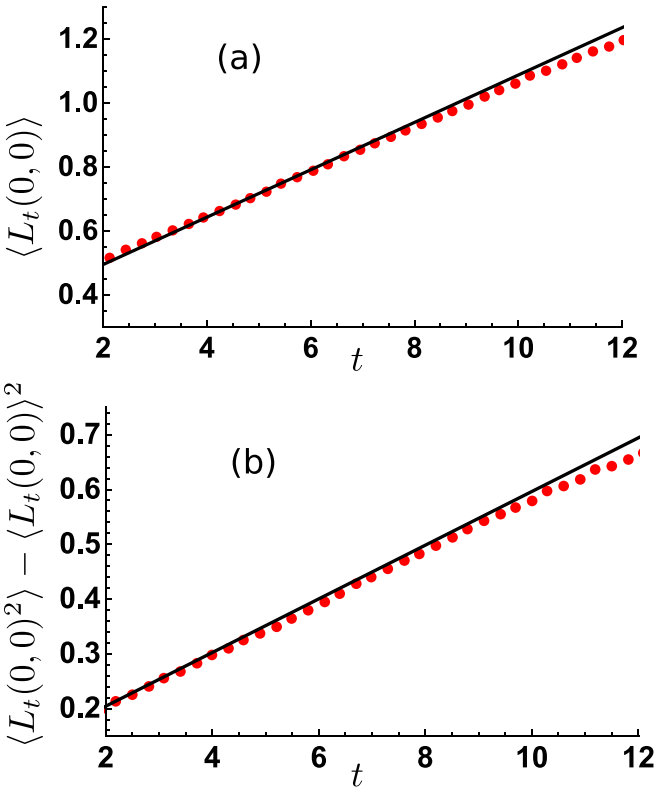

FIG. 4. Numerical verification of the growths of the mean (a) and the variance (b) of the local time L_t measured at the starting point $x_0 = y_0 = 0$ inside a box of length 2. The left side of the box is at the origin and is partially reflecting with parameter $\alpha_0 = 2$, whereas the right boundary is perfectly reflecting, $\alpha_L = 0$. The solid lines are obtained using Eqs. (B12)–(B23). Other parameters used in the simulation are $D = 1$ and $\Gamma = 10\,000$ (see Sec. V).

and, as a result, so does the the differential equation in Eq. (36). After writing its solution explicitly and then performing the inverse Laplace transforms we get for large t that (see Appendix B 1 for details)

$$P(L_t|x_0, 0, t) = \frac{1}{S(x_0, t)}\left[2\mathrm{erf}\left(\frac{x_0}{\sqrt{4Dt}}\right)\delta(L_t) + \sqrt{\frac{D}{\pi t}}e^{-\alpha_0 L_t D}e^{-\frac{(x_0+L_t D)^2}{4Dt}}\right], \tag{39}$$

and where

$$S(x_0, t) = e^{D\alpha_0^2 t + \alpha_0 x_0}\mathrm{erfc}\left(\frac{2D\alpha_0 t + x_0}{\sqrt{4Dt}}\right) + \mathrm{erf}\left(\frac{x_0}{\sqrt{4Dt}}\right). \tag{40}$$

The $\delta(L_t)$ term in Eq. (38) arises from those paths which are absorbed at the reactive boundary upon their first passage. The factor $\mathrm{erf}(x_0/\sqrt{4Dt})/S(x_0, t)$ represents the fraction of those paths, which starting at x_0 survived being absorbed by the reactive boundary and, moreover, did not make any visit to the boundary till time t. Note that this is the term that survives in the $\alpha_0 \to \infty$ limit, i.e., when the boundary becomes completely absorbing.

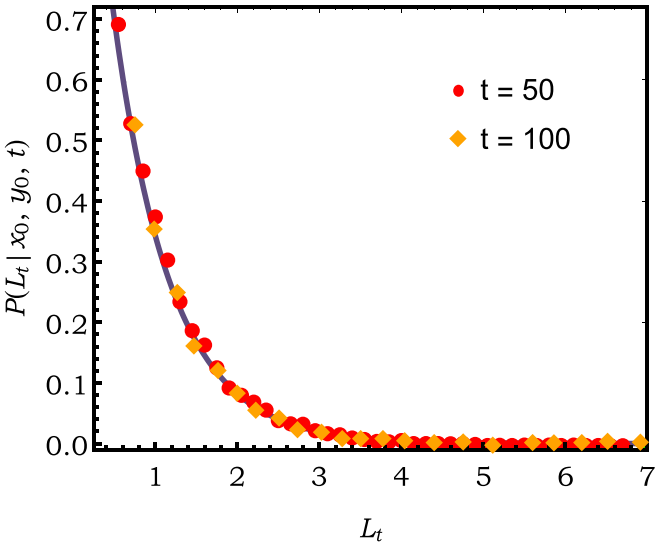

FIG. 5. Numerical distribution of local time L_t till the observation time t, starting from x_0. We measure the local time around its initial coordinate, $y_0 = x_0$, here. The point markers (circles and diamonds) represent simulation data obtained for time ($t = 50$ and 100, respectively). The solid line is obtained from the theoretical result in Eq. (41). Since Eq. (41) does not depend on t, we see all the data fall in the same line. The parameters for this figure are $D = 1$, $y_0 = x_0 = 0.5$, and $\alpha_0 = 5.0$.

A similar analysis for the case $y_0 = x_0$ reveals that the the asymptotic behavior for large t is given by (see Appendix B)

$$P(L_t|x_0, x_0, t)|_{t\to\infty} \simeq \frac{D\alpha_0}{1 + x_0\alpha_0}\, e^{-\frac{\alpha_0 D}{1+x_0\alpha_0}L_t}. \tag{41}$$

Note that the distribution of the local time becomes independent of time in the asymptotic limit of large t. In Fig. 5 we have compared the analytical expression of $P(L_t|x_0, x_0, t)$ given by Eq. (41) to the density obtained from the direct simulation of the Langevin equation. We see a nice agreement between them, and, moreover, we indeed observe that the densities are independent of t, as predicted from Eq. (41). On the other hand, for short times one obtains instead

$$P(L_t|x_0, x_0, t)|_{t\to 0} \simeq \sqrt{\frac{D}{\pi t}}\, e^{-\frac{L_t^2 D}{4t}}. \tag{42}$$

Note that the above expression is independent of the reactive constant α_0, since, for short times, the system is yet to see the boundaries and would behave like a free diffusion [54].

Local time density spent till the absorption time t_a

In the preceding section, we have studied the local time density spent by a Brownian molecule for a specific location over a fixed duration t. It may, however, occur that the molecule is absorbed before the reaction takes place (with zero contribution to the local time profile) or the reaction occurs with an immediate absorption. This motivates us to study the local time profile till the adsorption event. Since the absorption time is a functional of the trajectory, the local time density gets random contributions from two stochastic terms: the noise and the random absorption time.

Let us define the local time (density) $L_a(y_0, x_0)$ till the absorption event as

$$L_a(y_0, x_0) = \int_0^{t_a} \delta[x(t) - y_0|x_0]\, dt, \tag{43}$$

where t_a is the time when the molecule is absorbed at the boundary 0 and the initial condition is set as $x(0) = x_0$. As mentioned in Sec. II, the time t_a is a stochastic quantity, and this kind of functional is often known as the first passage time functionals in the literature [43]. It will prove convenient to rewrite the local time $L_a(y_0, x_0)$ in the following way:

$$L_a(y_0, x_0) = \lim_{\nu\to 0} \frac{W_\nu(y_0, x_0)}{2\nu}, \tag{44}$$

where

$$W_\nu(y_0, x_0) = \int_0^{t_a} V[x(t)]\, dt, \tag{45}$$

with

$$V(x) = \Theta[y_0 + \nu - x]\Theta[x - y_0 + \nu]. \tag{46}$$

The function $\Theta[x]$ is the Heaviside step function. Notice that the limit $\nu \to 0$, the function $V(x)$ corresponds to representing the Dirac delta $\delta(x - y_0)$ by a box of height $1/2\nu$ and width 2ν. Hence taking $\nu \to 0$ justifies our construction in Eq. (44) along with Eq. (45).

As done in the previous section, we start once again with the generating function $Q_\nu(p, y_0, x_0)$ of $W_\nu(y_0, x_0)$, which is defined as

$$Q_\nu(p, y_0, x_0) = \langle e^{-pW_\nu(y_0,x_0)}\rangle = \langle e^{-p\int_0^{t_a} V(x(t))dt}\rangle. \tag{47}$$

The generating function $\mathcal{T}_p(y_0, x_0)$ associated to L_a is equivalently defined as

$$\mathcal{T}_p(y_0, x_0) = \langle e^{-pL_a(y_0,x_0)}\rangle_{x_0} = \langle e^{-p\int_0^{t_a} \delta[x(t)-y_0|x_0]dt}\rangle. \tag{48}$$

Both generating functions are related to each other by

$$\mathcal{T}_p(y_0, x_0) = \lim_{\nu\to 0} Q_\nu(p/2\nu, y_0, x_0). \tag{49}$$

Using the Markov property one can show [43] that $Q_\nu(p, y_0, x_0)$ satisfies the following differential equation:

$$D\frac{d^2 Q_\nu}{dx_0^2} - p\, V(x_0)\, Q_\nu = 0, \tag{50}$$

which is accompanied by the following boundary conditions: as $x_0 \to \infty$, the time t_a to get absorbed also tends to infinity, which implies that $Q_\nu(p, y_0, x_0)$ cannot diverge and, second, at $x = 0$, we have a reactive boundary, which implies that

$$\left[\frac{dQ_\nu}{dx_0} - \alpha_0\, Q_\nu(p, y_0, x_0)\right]_{x_0=0} = -\alpha_0. \tag{51}$$

After some lengthy algebra,whose details can be found in Appendix C, one is able to obtain the following expression

for $P(L_a, y_0, x_0)$:

$$P(L_a, y_0, x_0) = \begin{cases} \frac{2\alpha_0(y_0-x_0)}{1+\alpha_0 y_0}\delta(L_a) + \alpha_0 D \frac{1+\alpha_0 x_0}{(1+\alpha_0 y_0)^2} e^{-\frac{\alpha_0 D}{1+\alpha_0 y_0}L_a}, & \text{if } 0 \leqslant x_0 \leqslant y_0, \\ \frac{\alpha_0 D}{(1+\alpha_0 y_0)} e^{-\frac{\alpha_0 D}{1+\alpha_0 y_0}L_a}, & \text{if } x_0 \geqslant y_0. \end{cases} \tag{52}$$

In the above expression we see that there is a δ-function contribution to the distribution of L_a. This results from those paths which are absorbed at the boundary before making a first passage to y_0. For this reason, the δ-function contribution appears only when $0 \leqslant x_0 \leqslant y_0$ or, in other words, there is a chance for the molecule to be absorbed at the boundary at $x = 0$ before ever reaching y_0 for the first time. This element of chance decreases as one starts closer to y_0, which explains the multiplicative factor $(y_0 - x_0)$. On the other hand, if the molecule starts at $x_0 \geqslant y_0$ it will definitely cross y_0 before it is absorbed at $x = 0$, and, as a result, it spends some nonzero time around y_0 (due to the Brownian nature of the motion). This is the reason behind the absence of a δ-function term for $x_0 \geqslant y_0$. In Fig. 6 we compare the analytical expression given by Eq. (52) to simulation results finding, once again, an excellent agreement.

V. METHODS OF SIMULATIONS

In this section, we outline the method we have used to simulate our system. There are many ways to generate trajectories of a Brownian particle diffusing in a box with two reactive boundaries [13,28,61,62]. In one such method, as described in Ref. [28], the authors define the partially reflected process as the limit of a Markovian jump process generated by the dynamics using an Euler scheme. Using boundary layer analysis, they derive a relation between the reactive constants and the reflection probability. In another paper [13], the authors study four different approaches to simulate such systems, and they have derived the correct choices of the reactive boundary conditions to implement in stochastic simulations. For our work, we have adapted one of these approaches from Ref. [13] to generate the trajectories. This is known as the Euler scheme for the velocity jump process [13]. In this scheme, one simulates the system by defining an auxiliary underdamped motion (by introducing a velocity component along with the existing position component) with a large friction coefficient Γ. The dynamics is discrete in time, continuous in space, and discontinuous in velocities. We sketch the basic steps in the following discussion.

Let us consider a system of N independent molecules. The ith molecule is described by two variables: its position $x_i(t)$ and velocity $v_i(t)$ at time t. The underdamped dynamics for the set $\{x_i(t), v_i(t)\}$ at each time step Δt is introduced in the following way:

$$\begin{aligned} x_i(t+\Delta t) &= x_i(t) + v_i(t)\Delta t, \\ v_i(t+\Delta t) &= v_i(t) - \Gamma v_i(t)\Delta t + \Gamma\sqrt{2D\Delta t}\eta_i, \end{aligned} \tag{53}$$

where Γ should be taken large and η_i is a normally distributed random variable with zero mean and unit variance [13]. In this problem we have two reactive boundaries at $x = 0$ and $x = L$, and the reactive boundary conditions can be stated as follows: whenever a molecule hits any one of the two boundaries $(0, L)$ it is adsorbed with probability $p_0/\sqrt{\Gamma}$ or $p_L/\sqrt{\Gamma}$, respectively, or reflected otherwise. The implementation is the following: whenever the value $x_i(t + \Delta t)$ computed from Eq. (53) is

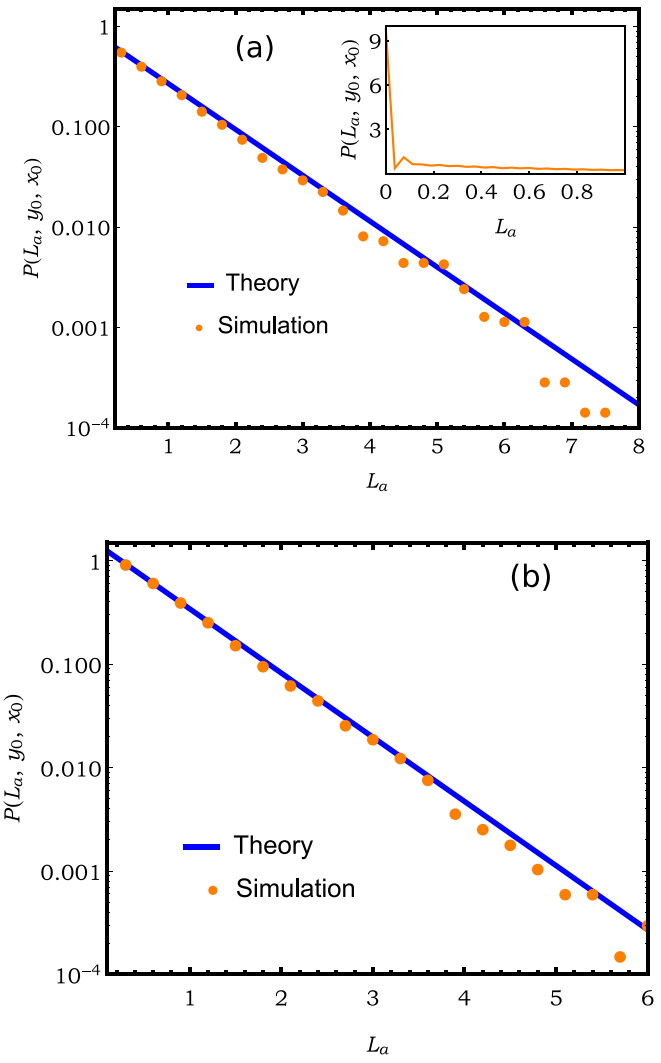

FIG. 6. Numerical distribution of the local time $P(L_a, y_0, x_0)$ at y_0 till its first adsorption at 0 given that it had started from x_0. We have compared the numerical simulation with the distribution obtained analytically in Eq. (52). The distribution has different analytical forms depending on x_0, y_0. In panel (a), we consider $x_0 = 0.5, y_0 = 0.75$ (so that $x_0 < y_0$), while in panel (b) we have $x_0 = 0.75, y_0 = 0.5$ (so that $x_0 > y_0$). In both plots, analytical formulas (solid blue lines) are plotted against the simulation curves (marked with orange circles). The inset in the left panel shows the presence of the Dirac δ function when $x_0 < y_0$. The parameters for this figure are set as $D = 1, \alpha_0 = 5.0$.

negative, then

$$x_i(t+\Delta t) = -x_i(t) - v_i(t)\Delta t,$$
$$v_i(t+\Delta t) = -v_i(t) + \Gamma v_i(t)\Delta t - \Gamma\sqrt{2D\Delta t}\,\eta_i, \quad (54)$$

with probability $1 - \frac{p_0}{\sqrt{\Gamma}}$, or we remove the ith molecule from the system. On the other hand, if $x_i(t+\Delta t)$ computed from Eq. (53) is greater than L, we do the following:

$$x_i(t+\Delta t) = 2L - x_i(t) - v_i(t)\Delta t,$$
$$v_i(t+\Delta t) = -v_i(t) + \Gamma v_i(t)\Delta t - \Gamma\sqrt{2D\Delta t}\,\eta_i, \quad (55)$$

with probability $1 - \frac{p_L}{\sqrt{\Gamma}}$; otherwise we remove the ith molecule from the system. Finally, we use the following relation between the reactive constants and the reflection probabilities [13]:

$$p_0 = \frac{\alpha_0\sqrt{2\pi}}{\sqrt{D}},$$
$$p_L = \frac{\alpha_L\sqrt{2\pi}}{\sqrt{D}}. \quad (56)$$

It is important that only in the high friction limit, that is, only when Γ is large enough, do we recover the diffusion equation (1), which is the overdamped limit and the inception of our study. Further details on how to prove this result can be found in Ref. [13]. In our particular case, we have taken $\Gamma = 500$ for all the simulations unless specified in particular case. The above prescription allows us to successfully generate Brownian trajectories in the presence of two reactive boundaries, and the number of molecules present in the system after a given time t is simply proportional to the probability density defined in Eq. (1). We conclude this section by stating that other statistical quantities such as the survival probability or the local time profile also can be simulated using this method.

VI. CONCLUSIONS AND FUTURE OUTLOOK

In this paper, we have provide a comprehensive study of various statistical properties of a Brownian molecule in the presence of reactive boundaries. Such boundaries are ubiquitous in physics, chemistry, and biology. Several molecular movements inside a cell can fairly well be described by a Brownian motion where the cell boundary provides the confined geometry. One often considers these boundaries to be either completely reflecting or completely absorbing. However, the effects of adsorption, catalysis, etc., occurring at the cell boundary makes them reactive, in the sense that these boundaries are neither fully absorbing nor fully reflecting. In this paper, we have looked at the Brownian motion of a molecule in one dimension with partially absorbing (reflecting) boundaries. We have also looked at the survival properties of the molecule, which also provides explicit expressions of the distribution of absorption time and the mean absorption time as well as the distribution of the maximum displacement. Using the Feynman-Kac formalism, we have investigated the distribution of the reaction or local time density both when observed for a fixed time or till the absorption time. We have obtained explicit expressions of the distribution of the local time which give an excellent match with the numerical simulations.

Our work can be extended in multiple directions. In a recent study [63], the authors considered the mean first passage time to a reaction event on a specific site in a cylindrical geometry with mixed boundary conditions. It would be interesting to estimate the survival probabilities and the longest excursions (maximum displacement and time to reach the maximum) in such a setup and further extend it to different nonuniform geometries. It would be also interesting to see how the properties of a tagged particle in the presence of other particles are effected by considering reactive crossing conditions. Effects of a partially absorbing boundary have also been investigated recently in an interesting stochastic dynamics, namely, stochastic resetting [64–69] which mixes long-range moves along with the local moves due to diffusion [50]. Moreover, such dynamics could be quite beneficial strategies to target searches [70,71]. It would be interesting to combine this dynamics in conjugation with diffusion to expedite first passage processes to a target in a confined domain with reactive boundaries.

ACKNOWLEDGMENTS

A.P. gratefully acknowledges support from the Raymond and Beverly Sackler Post-Doctoral Scholarship at Tel-Aviv University. A.K. acknowledges support from DST grant under project No. ECR/2017/000634. This work benefited from the support of the project 5604-2 of the Indo-French Centre for the Promotion of Advanced Research (IFCPAR). We would also like to thank the Weizmann Institute of Science for the hospitality during the SRitp workshop where part of this work was done. I.P.C thanks the Laboratoire de Physique Théorique et Modèles Statistiques (Université de Paris-Sud), where this work was initiated, for its hospitality.

APPENDIX A: DERIVATIONS OF THE PROPAGATOR IN THE SEMI-INFINITE DOMAIN

To derive the propagator in the semi-infinite domain, we have to take the limit $L \to \infty$ in Eq. (4). In this limit Eq. (5) yields $k = \frac{n\pi}{L}$. The summation over k can now be converted into an integral over k as $L \to \infty$. A short calculation gives us

$$\begin{aligned} G_t^{\rm si}(x,x_0) &= \frac{1}{2\pi}\left[\frac{\partial}{\partial x}\frac{\partial}{\partial x_0} + \alpha_0\left(\frac{\partial}{\partial x} + \frac{\partial}{\partial x_0}\right) + \alpha_0^2\right] \\ &\quad \times \int_{-\infty}^{\infty} dk\, \frac{2\sin(kx_0)\sin(kx)}{\alpha_0^2 + k^2}\, e^{-Dk^2t} \\ &= \frac{1}{2\pi}\left(\frac{\partial}{\partial x} + \alpha_0\right)\left(\frac{\partial}{\partial x_0} + \alpha_0\right) \\ &\quad \times \int_{-\infty}^{\infty} dk\, \frac{\cos[k(x+x_0)] + \cos[k(x-x_0)]}{\alpha_0^2 + k^2} \\ &\quad \times e^{-Dk^2t}. \end{aligned} \quad (A1)$$

To compute Eq. (A1) we consider the following integral:

$$\begin{aligned} I_\alpha(z) &= \int_{-\infty}^{\infty} dk \frac{\cos(kz)}{\alpha^2 + k^2} e^{-k^2t} \\ &= e^{\alpha^2 t}\left[\int_{-\infty}^{\infty} dk \frac{\cos(kz)}{\alpha^2 + k^2} e^{-(\alpha^2 + k^2)t}\right]. \end{aligned} \quad (A2)$$

By noting that $\int_t^\infty dt'\ e^{-(k^2+\alpha^2)t'} = \frac{e^{-(\alpha^2+k^2)t}}{\alpha^2+k^2}$, we find from Eq. (A2)

$$I_\alpha(z) = e^{\alpha^2 t}\int_t^\infty dt' e^{-\alpha^2 t'}\mathrm{Re}\left[\int_{-\infty}^{\infty} dk e^{ikz} e^{-k^2 t'}\right] = \frac{2\sqrt{\pi}}{\alpha} e^{y^2}\int_y^\infty dq e^{-q^2} e^{-\frac{z^2\alpha^2}{4q^2}}, \tag{A3}$$

where $y = \alpha\sqrt{t}$. Applying the standard integral formula

$$\int_y^\infty dt e^{-a^2t^2-\frac{b^2}{t^2}} = \frac{\sqrt{\pi}}{4a} e^{2ab}\mathrm{erfc}\left[ay + \frac{b}{y}\right] + \frac{\sqrt{\pi}}{4a} e^{-2ab}\mathrm{erfc}\left[ay - \frac{b}{y}\right], \tag{A4}$$

in Eq. (A3), eventually we obtain from Eq. (A2)

$$I_\alpha(z) = \frac{\pi}{2\alpha} e^{\alpha^2 t}\left[e^{z\alpha}\mathrm{erfc}\left(\frac{2\alpha t + z}{\sqrt{4t}}\right) + e^{-x_0\alpha}\mathrm{erfc}\left(\frac{2\alpha t - z}{\sqrt{4t}}\right)\right]. \tag{A5}$$

Plugging the above expression in Eq. (A1), we obtain Eq. (6) along with Eq. (7).

APPENDIX B: DERIVATIONS OF STATISTICAL PROPERTIES OF LOCAL TIME SPENT AT y_0 TILL OBSERVATION TIME t

In this Appendix we present the detailed derivations regarding the statistical properties of local time spent at y_0 till observation time t. Starting from Eq. (36), we notice that one can write its solution into two separate regions:

$$\tilde{Q}_p^{(I)}(y_0, x_0, s) = A_1 e^{-x_0\sqrt{s/D}} + B_1 e^{x_0\sqrt{s/D}} + \frac{1}{s}, \tag{B1}$$

for $\leqslant x_0 \leqslant y_0$, and

$$\tilde{Q}_p^{(II)}(y_0, x_0, s) = A_2 e^{-x_0\sqrt{s/D}} + B_2 e^{x_0\sqrt{s/D}} + \frac{1}{s}, \tag{B2}$$

for $y_0 \leqslant x_0 \leqslant L$. The constants $A_1, A_2, B_1,$ and B_2 are fixed by implementing the boundary conditions (37), together with continuity of the solution at $x_0 = y_0$, and discontinuity of the first derivative at $x_0 = y_0$. These conditions yield

$$\frac{\alpha_0}{s} = B_1(\sqrt{s/D} - \alpha_0) - A_1(\sqrt{s/D} + \alpha_0), \tag{B3}$$

$$-\frac{\alpha_L}{s} = B_2(\sqrt{s/D} + \alpha_L)e^{L\sqrt{s/D}} - A_2(\sqrt{s/D} - \alpha_L)e^{-L\sqrt{s/D}}, \tag{B4}$$

$$B_1 e^{y_0\sqrt{s/D}} + A_1 e^{-y_0\sqrt{s/D}} = A_2 e^{-y_0\sqrt{s/D}} + B_2 e^{y_0\sqrt{s/D}}, \tag{B5}$$

$$\frac{p}{sD} = -\sqrt{\frac{s}{D}}\,A_2 e^{-y_0\sqrt{s/D}} + \sqrt{\frac{s}{D}}\,B_2 e^{y_0\sqrt{s/D}} + \left(\sqrt{\frac{s}{D}} - \frac{p}{D}\right)A_1 e^{-y_0\sqrt{s/D}} - \left(\sqrt{\frac{s}{D}} + \frac{p}{D}\right)B_1 e^{y_0\sqrt{s/D}}. \tag{B6}$$

For later use, it is convenient to introduce the following function:

$$\tilde{R}_L(s) = \sqrt{s}[p + D(\alpha_0 + \alpha_L)]\cosh\left[\frac{L\sqrt{s}}{\sqrt{D}}\right] + \sqrt{D}[s + (p + \alpha_0 D)\alpha_L]\sinh\left[\frac{L\sqrt{s}}{\sqrt{D}}\right]. \tag{B7}$$

Particularizing for an initial position set at $y_0 = 0$, we obtain the following solution for the four constants A_1, A_2, B_1, and B_2:

$$4\,A_1\,\sqrt{s}\sqrt{\frac{s}{D}}\,\tilde{R}_L(s) = e^{-L\sqrt{\frac{s}{D}}}\left\{ - p\left[e^{2L\sqrt{\frac{s}{D}}}\left(\sqrt{\frac{s}{D}} + \alpha_L\right) + \sqrt{\frac{s}{D}} - \alpha_L\right] - 2De^{L\sqrt{\frac{s}{D}}}\left[\alpha_0 e^{L\sqrt{\frac{s}{D}}}\left(\sqrt{\frac{s}{D}} + \alpha_L\right) - \alpha_L\left(\alpha_0 - \sqrt{\frac{s}{D}}\right)\right]\right\}, \tag{B8}$$

$$2\sqrt{D}\,s\,A_2\left(\sqrt{\frac{s}{D}} - \alpha_0\right)\tilde{R}_L(s) = \left\{-D\alpha_L\left[s + \alpha_0 D\left(-2\sqrt{\frac{s}{D}} + \alpha_0\right) + p\left(-\sqrt{\frac{s}{D}} + \alpha_0\right)\right] + e^{L\sqrt{\frac{s}{D}}}(p + D\alpha_0)\left[-s + D\left(\sqrt{\frac{s}{D}}\alpha_0 - \sqrt{\frac{s}{D}}\alpha_L + \alpha_0\alpha_L\right)\right]\right\}, \tag{B9}$$

$$2sB_1\left(s - \alpha_0 D\sqrt{\frac{s}{D}}\right)\tilde{R}_L(s) = e^{-L\sqrt{\frac{s}{D}}}\left(D\sqrt{s}\left[-\alpha_L(s - \alpha_0^2 D)e^{L\sqrt{\frac{s}{D}}} + \alpha_0\alpha_L\sqrt{sD} + \alpha_0(-\alpha_0 D\alpha_L - s) + \alpha_0^2\sqrt{sD}\right] - \left\{pe^{L\sqrt{\frac{s}{D}}}\left(s - \alpha_0 D\sqrt{\frac{s}{D}}\right)\left[\sqrt{s}\cosh\left(\frac{L\sqrt{s}}{\sqrt{D}}\right) + \sqrt{D}\alpha_L\sinh\left(\frac{L\sqrt{s}}{\sqrt{D}}\right)\right]\right\}\right), \tag{B10}$$

$$2B_2\,\sqrt{s}(s - \sqrt{sD}\alpha_0)\,\tilde{R}_L(s) = e^{-L\sqrt{\frac{s}{D}}}\left\{p\sqrt{sD}\alpha_0 + D^2\sqrt{\frac{s}{D}}\,\alpha_0^2 + p\sqrt{sD}\alpha_L - p\sqrt{sD}\alpha_L\,e^{L\sqrt{\frac{s}{D}}} + D^2\sqrt{\frac{s}{D}}\alpha_0\alpha_L - D\alpha_L\,e^{L\sqrt{\frac{s}{D}}}[s - \alpha_0(p + D\alpha_0)] + (p + D\alpha_0)(-s - D\alpha_0\alpha_L)\right\}. \tag{B11}$$

As mentioned earlier, at this stage it is hard to perform the inverse Laplace transform on $\tilde{Q}_p(0, x_0, s)$ to obtain $\tilde{\mathcal{Q}}_p(0, x_0, t)$. Instead, we compute the first and the second moment of the local time from $\tilde{Q}_p(0, x_0, s)$. First, note that

$$\langle L_t(0,x_0)\rangle = -\frac{1}{S_L(x_0,t)}\frac{\partial Q_p(0,x_0,t)}{\partial p}\bigg|_{p\to 0} = \frac{\langle l_t(0,x_0)\rangle}{S_L(x_0,t)},$$
$$\left\langle L_t^2(0,x_0)\right\rangle = \frac{1}{S_L(x_0,t)}\frac{\partial^2 Q_p(0,x_0,t)}{\partial p^2}\bigg|_{p\to 0} = \frac{\left\langle l_t^2(0,x_0)\right\rangle}{S_L(x_0,t)}, \tag{B12}$$

where $S_L(x_0,t)$ is the associated survival probability given by Eq. (9) and we have defined

$$\langle l_t(0,x_0)\rangle \equiv -\frac{\partial Q_p(0,x_0,t)}{\partial p}\bigg|_{p\to 0}, \tag{B13}$$
$$\left\langle l_t^2(0,x_0)\right\rangle \equiv \frac{\partial^2 Q_p(0,x_0,t)}{\partial p^2}\bigg|_{p\to 0}. \tag{B14}$$

Now, we can take the Laplace transform on $\langle l_t(0,x_0)\rangle$ and $\langle l_t^2(0,x_0)\rangle$, which is related to $\tilde{\mathcal{Q}}_p(0,x_0,s)$ in the following manner:

$$f_1(s) \equiv \mathcal{L}_t[\langle l_t(0,x_0)\rangle] = -\frac{\partial \tilde{Q}_p(0,x_0,s)}{\partial p}\bigg|_{p\to 0}, \tag{B15}$$
$$f_2(s) \equiv \mathcal{L}_t\left[\left\langle l_t^2(0,x_0)\right\rangle\right] = \frac{\partial^2 \tilde{Q}_p(0,x_0,s)}{\partial p^2}\bigg|_{p\to 0}. \tag{B16}$$

We further simplify our calculations by taking both boundaries to be purely reflecting, $\alpha_0 = \alpha_L = 0$. Now defining $\tau_1 = \frac{L-x_0}{\sqrt{D}}$ and $\tau_2 = L/\sqrt{D}$, we can write

$$f_1(s) = \frac{\cosh(\tau_1\sqrt{s})}{\sqrt{D}s^{3/2}\sinh(\tau_2\sqrt{s})},$$
$$f_2(s) = \frac{2\cosh(\tau_1\sqrt{s})\cosh(\tau_2\sqrt{s})}{Ds^2\sinh(\tau_2\sqrt{s})^2}. \tag{B17}$$

Now we can do inverse Laplace transform on Eq. (B17) with respect to s to arrive at the following expressions:

$$\langle l_t(0,x_0)\rangle = \frac{1}{\sqrt{D}}\left[\frac{\tau_1^2}{2\tau_2} + \frac{t}{\tau_2} - \frac{\tau_2}{6} - 2\tau_2\sum_{n=1}^{\infty}\frac{(-1)^n}{n^2\pi^2}\cos\frac{n\pi\tau_1}{\tau_2}e^{-\frac{n^2\pi^2 t}{\tau_2^2}}\right] \tag{B18}$$

and

$$\left\langle l_t^2(0,x_0)\right\rangle = \frac{\tau_1^2}{6D} + \frac{\tau_1^4}{12\tau_2^2 D} - \frac{7\tau_2^2}{60D} + \frac{t}{3D} + \frac{\tau_1^2 t}{\tau_2^2 D} + \frac{t^2}{\tau_2^2 D} - \frac{4}{D}\sum_{n=1}^{\infty}\frac{(-1)^n e^{-\frac{n^2\pi^2 t}{\tau_2^2}}}{n^4\pi^4}\left[\tau_1\tau_2 n\pi\sin\frac{n\pi\tau_1}{\tau_2} + \left(3\tau_2^2 + 2n^2\pi^2 t\right)\cos\frac{n\pi\tau_1}{\tau_2}\right]. \tag{B19}$$

Similarly, when $\alpha_L = 0, \alpha_0 \neq 0$, after a lengthy calculation we find

$$\int_0^\infty dt e^{-st}\langle l_t(0,x_0)\rangle = \frac{\cosh\tau_1\sqrt{s}}{\sqrt{D}}\frac{\sinh\tau_2\sqrt{s}/\sqrt{s}}{(\sqrt{s}\sinh\tau_2\sqrt{s} + \sqrt{D}\alpha_0\cosh\tau_2\sqrt{s})^2} \tag{B20}$$

and

$$\int_0^\infty dt\ e^{-st}\left\langle l_t^2(0,x_0)\right\rangle = \frac{\cosh^2\tau_1\sqrt{s}}{\sqrt{D}} \tag{B21}$$
$$\times\frac{\sinh\tau_2\sqrt{s}/\sqrt{s}}{(\sqrt{s}\sinh\tau_2\sqrt{s} + \sqrt{D}\alpha_0\cosh\tau_2\sqrt{s})^3}. \tag{B22}$$

The inversion of these expression can be done analytically; however, it is not possible to express this inversion in explicit forms, because the zeros of this expression come from solutions of the transcendental equation

$$\tau_2\sqrt{s}\tanh\tau_2\sqrt{s} = -\alpha_0 L, \tag{B23}$$

which one can compute numerically rather easily. One finds that the poles lie on the negative real axis. Since poles occurs at these zeros and since they are simple multiple order poles, one can just evaluate the residues while performing the Bromwich integral. In the large t limit, it is enough to compute the contribution from the largest pole, i.e., the one which lies closest to the origin on the negative real axis. For large $L > 3/\alpha_0$, one can solve the transcendental equation in (B23) to find an approximate form of this pole for $x_0 = 0$, which is given by

$$s_0 = -\frac{\pi^2 D}{4L^2} + \frac{\pi^2 D}{3L^2 + \alpha_0 L^3}. \tag{B24}$$

A comparison of the analytical results with simulation for the mean and variance obtained following the above procedure is given in the main text (see Fig. 4). For both $\alpha_0 \neq 0$ and $\alpha_L \neq 0$, one can proceed in the same way to compute various cumulants. The calculations are straightforward but fairly lengthy.

1. Semi-infinite case: $L \to \infty$

The calculation for the distribution of L_t becomes simpler in the semi-infinite case, in the $L \to \infty$ limit. We first consider $y_0 = 0$, and we start from

$$\mathcal{Q}_p(y_0,x_0,t) = \frac{Q_p(y_0,x_0,t)}{S(x_0,t)}, \tag{B25}$$
$$Q_p(y_0,x_0,t) = \int_0^\infty dx\langle x|e^{-t\hat{H}_p}|x_0\rangle, \tag{B26}$$

where $S(x_0,t)$ is given by Eq. (10), while the governing equation for $\tilde{Q}_p(y_0,x_0,s)$ is still given by Eq. (34) with new boundary conditions:

$$\left[\frac{\partial\tilde{Q}_p}{\partial x_0} - \alpha_0\tilde{Q}_p\right]_{x_0=0} = 0,$$
$$\tilde{Q}_p(y_0,x_0,s)|_{x_0\to\infty} = \frac{1}{s}. \tag{B27}$$

The second boundary condition is obtained from the fact that as $x_0 \to \infty$, the local time $L_t \to 0$, which results in $Q_p \to 1$. To obtain a complete solution of $\tilde{Q}_p(y_0, x_0, s)$ of Eq. (34) with these new boundary conditions, we write the solution in the following regions:

$$\tilde{Q}_p^{(I)}(y_0, x_0, s) = A\, e^{-x_0\sqrt{s/D}} + B\, e^{x_0\sqrt{s/D}} + \frac{1}{s}, \quad \text{(B28)}$$

for $0 \leqslant x_0 \leqslant y_0$, and

$$\tilde{Q}_p^{(II)}(y_0, x_0, s) = C\, e^{-x_0\sqrt{s/D}} + \frac{1}{s}, \quad \text{(B29)}$$

for $x_0 \geqslant y_0$. The constants A, B, and C can be obtained imposing the following conditions: (a) boundary condition at $x_0 = 0$, (b) continuity of the solution at $x_0 = y_0$, and (c) discontinuity of the first derivative at $x_0 = y_0$. The first two yield

$$B(\sqrt{s/D} - \alpha_0) - A(\sqrt{s/D} + \alpha_0) = \frac{\alpha_0}{s}, \quad \text{(B30)}$$

$$Be^{y_0\sqrt{s/D}} + Ae^{-y_0\sqrt{s/D}} = Ce^{-y_0\sqrt{s/D}}, \quad \text{(B31)}$$

which can be solved to obtain an expression in terms of the constant C:

$$Ae^{-y_0\sqrt{s/D}} = \frac{\sqrt{D}}{2R_{y_0}(s)}\left[-\frac{\alpha}{s} + C\,(\sqrt{s/D} - \alpha_0)\, e^{-2y_0\sqrt{s/D}}\right], \quad \text{(B32)}$$

$$Be^{y_0\sqrt{s/D}} = \frac{\sqrt{D}}{2R_{y_0}(s)}\left[\frac{\alpha}{s} + C\left(\sqrt{\frac{s}{D}} + \alpha_0\right)\right], \quad \text{(B33)}$$

where we have defined the function

$$R_{y_0}(s) = \sqrt{s}\cosh\left(y_0\sqrt{\frac{s}{D}}\right) + \alpha_0\sqrt{D}\sinh\left(y_0\sqrt{\frac{s}{D}}\right). \quad \text{(B34)}$$

Finally, using these solutions into the third condition results into the following expression for the constant C:

$$C\, e^{-y_0\sqrt{s/D}} = -\frac{1}{s}\,\frac{pR_{y_0}(s) + \alpha_0 D\sqrt{s}}{pR_{y_0}(s) + \sqrt{s}(\sqrt{sD} + \alpha_0 D)\, e^{y_0\sqrt{s/D}}}. \quad \text{(B35)}$$

Thus we have a complete solution of $\tilde{Q}_p(y_0, x_0, s)$, from which performing double inverse Laplace transformation one can, in principle, obtain $P(L_t|x_0, y_0, t)$ for any reaction location y_0. In the following we consider two choices for this location to demonstrate few exact results. The choices are (1) at the origin ($y_0 = 0$) and (2) at its initial position $y_0 = x_0$.

For the first case ($y_0 = 0$), notice that the function $R_{y_0}(s) = \sqrt{s}$. Hence, the constant C in Eq. (B35) now reads

$$C = -\frac{1}{s}\,\frac{p + \alpha_0 D}{p + \alpha_0 D + \sqrt{sD}}, \quad \text{(B36)}$$

and as a result the function $\tilde{Q}_p(0, x_0, s)$ has the following form:

$$\begin{aligned}\tilde{Q}_p(0, x_0, s) &= \frac{1}{s} - \frac{1}{s}\,\frac{p + \alpha_0 D}{p + \alpha_0 D + \sqrt{sD}}\, e^{-x_0\sqrt{s/D}}, \\ &= \frac{1 - e^{-x_0\sqrt{s/D}}}{s} \\ &\quad + \frac{e^{-x_0\sqrt{s/D}}}{\sqrt{s}(p + \alpha_0 D + \sqrt{sD})}. \end{aligned} \quad \text{(B37)}$$

Performing the inverse Laplace transform with respect to s we obtain

$$\begin{aligned}Q_p(0, x_0, t) &= S(x_0, t)\mathcal{Q}_p(0, x_0, t) \\ &= e^{D\alpha_p^2 t + \alpha_p x_0}\mathrm{erfc}\left(\frac{2D\alpha_p t + x_0}{\sqrt{4Dt}}\right) + \mathrm{erf}\left(\frac{x_0}{\sqrt{4Dt}}\right), \end{aligned} \quad \text{(B38)}$$

where $\alpha_p = \alpha_0 + \frac{p}{D}$. Now performing the inverse Laplace transform with respect to p, we get

$$\begin{aligned}q_0(L_t, t|x_0) &= \mathcal{L}_{L_t}^{-1}[Q_p(0, x_0, t)] \\ &= 2\mathrm{erf}\left(\frac{x_0}{\sqrt{4Dt}}\right)\delta(L_t) \\ &\quad + \sqrt{\frac{D}{\pi t}}e^{-\alpha_0 L_t D}e^{-\frac{(x_0 + L_t D)^2}{4Dt}}. \end{aligned} \quad \text{(B39)}$$

Hence, the distribution of the local time (density) at $y_0 = 0$ is given by

$$\begin{aligned}P(L_t|x_0, 0, t) &= \frac{1}{S(x_0, t)}\left[2\mathrm{erf}\left(\frac{x_0}{\sqrt{4Dt}}\right)\delta(L_t)\right. \\ &\quad \left. + \sqrt{\frac{D}{\pi t}}e^{-\alpha_0 L_t D}e^{-\frac{(x_0 + L_t D)^2}{4Dt}}\right], \end{aligned} \quad \text{(B40)}$$

where

$$\begin{aligned}S(x_0, t) &= e^{D\alpha_0^2 t + \alpha_0 x_0}\mathrm{erfc}\left(\frac{2D\alpha_0 t + x_0}{\sqrt{4Dt}}\right) \\ &\quad + \mathrm{erf}\left(\frac{x_0}{\sqrt{4Dt}}\right), \end{aligned} \quad \text{(B41)}$$

and reported in the main text.

Let us consider now the second case, the local time around its initial position $y_0 = x_0$. Plugging $y_0 = x_0$ into Eqs. (B28) and (B29), and using the expression of C from Eq. (B35), we have

$$\begin{aligned}\tilde{Q}_p(x_0, x_0, s) &= \frac{1}{s} + Ce^{-x_0\sqrt{s/D}} \\ &= \frac{1}{s}\,\frac{s\sqrt{D} + \alpha_0 D\sqrt{s}(1 - e^{-y_0\sqrt{s/D}})}{R_{y_0}(s)e^{-x_0\sqrt{s/D}}} \\ &\quad \times \frac{1}{p + \frac{s\sqrt{D} + \alpha_0 D\sqrt{s}}{R_{x_0}(s)}e^{-x_0\sqrt{s/D}}}, \end{aligned} \quad \text{(B42)}$$

where $R_{x_0}(s)$ is given by Eq. (B34). Performing the inverse Laplace transform with respect to p we get

$$\begin{aligned}\tilde{Z}_s(L_t, x_0) &= \mathcal{L}_{L_t}^{-1}[\tilde{Q}_p(x_0, x_0, s)] \\ &= \frac{1}{s}\,\frac{s\sqrt{D} + \alpha_0 D\sqrt{s}(1 - e^{-x_0\sqrt{s/D}})}{R_{x_0}(s)e^{-x_0\sqrt{s/D}}} \\ &\quad \times e^{-\frac{s\sqrt{D} + \alpha_0 D\sqrt{s}}{R_{x_0}(s)}e^{-x_0\sqrt{s/D}}L_t}. \end{aligned} \quad \text{(B43)}$$

We need to perform another inverse Laplace transform with respect to s to get $Z_t(L_t, x_0) = \mathcal{L}_s^{-1}[\tilde{Z}_s(L_t, x_0)]$. We can then use this result to obtain the local time density $P(L_t|x_0, x_0, t)$ as

$$P(L_t|x_0, x_0, t) = \frac{Z_t(L_t, x_0)}{S(x_0, t)}, \tag{B44}$$

where $S(x_0, t)$ is the survival probability given by Eq. (B40). It is, however, rather cumbersome to perform the second Laplace inversion analytically. We can obtain analytical expressions in the limits for large and short times. Indeed, let us start consider the asymptotic behavior for large t. In this case, the dominant contribution to the inverse Laplace transform with respect to s comes from the small s limit of $\tilde{Z}_s(L_t, x_0)$, and that is given by

$$\tilde{Z}_s(L_t, x_0)|_{s\to 0} \simeq \sqrt{D}\, e^{-\frac{\alpha_0 D L_t}{1+x_0\alpha_0}}\, \frac{1}{\sqrt{s}}\, e^{-\frac{D L_t \sqrt{s}}{1+x_0\alpha_0}}, \tag{B45}$$

which provides

$$Z_t(L_t, x_0)|_{t\to\infty} \simeq \sqrt{\frac{D}{\pi t}}\, e^{-\frac{\alpha_0 D L_t}{1+x_0\alpha_0}}\, e^{-\frac{D^2 L_t^2}{4t(1+x_0\alpha_0)^2}}. \tag{B46}$$

On the other hand, $S(x_0, t)|_{t\to\infty} \simeq \frac{1+x_0\alpha_0}{\sqrt{\pi D t}\alpha_0^2}$. Hence the density function $P(L_t|x_0, x_0, t)$ for large t is given by

$$P(L_t|x_0, x_0, t)|_{t\to\infty} \simeq \frac{D\alpha_0}{1+x_0\alpha_0}\, e^{-\frac{\alpha_0 D}{1+x_0\alpha_0} L_t}. \tag{B47}$$

Note that the distribution of the local time becomes independent of time for asymptotically large t.

On the other side of the time variable, for small t, the dominant contribution to the inverse Laplace transform with respect to s comes from the large s limit of $\tilde{Z}_s(L_t, x_0)$ and that is given by

$$\tilde{Z}_s(L_t, x_0)|_{s\to\infty} \simeq \sqrt{D}\, \frac{e^{-L_t\sqrt{sD}}}{\sqrt{s}}, \tag{B48}$$

which yields

$$Z_t(L_t, x_0)|_{t\to 0} \simeq \sqrt{\frac{D}{\pi t}}\, e^{-\frac{L_t^2 D}{4t}}. \tag{B49}$$

In this case $S(x_0, t)|_{t\to 0} \simeq 1 - \frac{4\alpha_0 (Dt)^{3/2}}{\sqrt{\pi}\, x_0^2}\, e^{-\frac{x_0^2}{4Dt}}$. Therefore, the density function $P(L_t|x_0, x_0, t)$ for small t reads

$$P(L_t|x_0, x_0, t)|_{t\to 0} \simeq \sqrt{\frac{D}{\pi t}}\, e^{-\frac{L_t^2 D}{4t}}, \tag{B50}$$

as reported in the main text.

APPENDIX C: DERIVATION OF $P(L_a, y_0, x_0)$

To find a solution of the differential equation (50) we first notice that this is naturally divided in three different regions: (1) $0 \leqslant x_0 \leqslant y_0 - \nu$, (2) $y_0 - \nu \leqslant x_0 \leqslant y_0 + \nu$, and (3) $x_0 \geqslant y_0 + \nu$. Thus, the solution can be written in the following way:

$$Q_\nu(p, y_0, x_0) = A_\nu + B_\nu\, x_0, \quad \text{for} \quad 0 \leqslant x_0 \leqslant y_0 - \nu, \tag{C1}$$

$$Q_\nu(p, y_0, x_0) = F_\nu\, \cosh\left[(x_0 - y_0 - \nu)\sqrt{\frac{p}{D}}\right], \quad \text{for} \quad y_0 - \nu \leqslant x_0 \leqslant y_0 + \nu, \tag{C2}$$

$$Q_\nu(p, y_0, x_0) = F_\nu, \quad \text{for} \quad x_0 \geqslant y_0 + \nu. \tag{C3}$$

The constants A_ν, B_ν, and F_ν are computed from the following matching conditions: (a) continuity of the solutions, (b) continuity of their derivatives at $x_0 = y_0 \pm \nu$, and (c) using the reactive boundary condition at $x_0 = 0$ according to Eq. (51). Now, using the matching conditions (a) and (b) yields

$$A_\nu + B_\nu(y_0 - \nu) - F_\nu\, \cosh\left[2\nu\sqrt{\frac{p}{D}}\right] = 0, \tag{C4}$$

$$B_\nu(y_0 - \nu)\sqrt{D} + \sqrt{p}F_\nu\, \sinh\left[2\nu\sqrt{\frac{p}{D}}\right] = 0. \tag{C5}$$

Similarly, the boundary condition (c) at $x_0 = 0$ allows us to write

$$B_\nu = \alpha_0\, A_\nu - \alpha_0. \tag{C6}$$

Solving the three equations (C4), (C5), and (C6), we get

$$A_\nu(p) = \alpha_0\, \frac{(y_0 - \nu)\sqrt{p}\sinh(2\nu\sqrt{p/D}) + \sqrt{D}\cosh(2\nu\sqrt{p/D})}{[1 + \alpha_0(y_0 - \nu)]\sqrt{p}\sinh(2\nu\sqrt{p/D}) + \alpha_0\sqrt{D}\cosh(2\nu\sqrt{p/D})}, \tag{C7}$$

$$B_\nu(p) = -\alpha_0\, \frac{\sqrt{p}\sinh(2\nu\sqrt{p/D})}{[1 + \alpha_0(y_0 - \nu)]\sqrt{p}\sinh(2\nu\sqrt{p/D}) + \alpha_0\sqrt{D}\cosh(2\nu\sqrt{p/D})}, \tag{C8}$$

$$F_\nu(p) = \frac{\alpha_0\sqrt{D}}{[1 + \alpha_0(y_0 - \nu)]\sqrt{p}\sinh(2\nu\sqrt{p/D}) + \alpha_0\sqrt{D}\cosh(2\nu\sqrt{p/D})}. \tag{C9}$$

To establish the connection between the generating function as prescribed in Eq. (49), we first take the $\nu \to 0$ limit in the expressions of the constants $A_\nu(p/2\nu)$, $B_\nu(p/2\nu)$, and $F_\nu(p/2\nu)$. This yields

$$A_a = \lim_{\nu\to 0} A_\nu(p/2\nu) = \frac{\alpha_0(y_0 p + D)}{(1 + \alpha_0 y_0)p + \alpha_0 D}, \tag{C10}$$

$$B_a = \lim_{\nu\to 0} B_\nu(p/2\nu) = -\frac{\alpha_0 p}{(1 + \alpha_0 y_0)p + \alpha_0 D}, \tag{C11}$$

$$F_a = \lim_{\nu\to 0} F_\nu(p/2\nu) = \frac{\alpha_0 D}{(1 + \alpha_0 y_0)p + \alpha_0 D}. \tag{C12}$$

All in all, we arrive at the following solution of the generating function $\mathcal{T}_p(y_0, x_0)$:

$$\mathcal{T}_p(y_0, x_0) = \begin{cases} \frac{p\alpha_0(y_0 - x_0) + \alpha_0 D}{(1+\alpha_0 y_0)p + \alpha_0 D}, & \text{if } 0 \leqslant x_0 \leqslant y_0, \\ \frac{\alpha_0 D}{(1+\alpha_0 y_0)p + \alpha_0 D}, & \text{if } x_0 \geqslant y_0. \end{cases} \tag{C13}$$

Finally, to obtain the distribution $P(L_a, y_0, x_0)$ we need to perform the inverse Laplace transform in Eq. (C13), which yields the full distribution $P(L_a, y_0, x_0)$ given by Eq. (52).

[1] A. N. Borodin and P. Salminen, *Handbook of Brownian Motion-Facts and Formulae* (Birkhäuser, Basel, 2012).
[2] H. Berg, *Random Walks in Biology* (Princeton University Press, Princeton, 1983).
[3] J. Crank, *The Mathematics of Diffusion* (Oxford University Press, Oxford, 1975).
[4] G. M. Cooper and R. E. Hausman, *The Cell: A Molecular Approach*, 7th ed. (Sinauer Associates, Sunderland, MA, 2016).
[5] L. Vroman, A. L. Adams, G. C. Fischer, and P. C. Munoz, Blood **55**, 156 (1980); J. L. Brash *et al.*, *ibid.* **71**, 932 (1988); J. G. Donaldson, R. A. Kahn, J. Lippincott-Schwartz, and R. D. Klausner, Science **254**, 1197 (1991).
[6] O. V. Bychuk and B. O'Shaughnessy, Phys. Rev. Lett. **74**, 1795 (1995); R. Valiullin, R. Kimmich, and N. Fatkullin, Phys. Rev. E **56**, 4371 (1997).
[7] D. S. Grebenkov, in *Focus on Probability Theory*, ed. L. R. Velle (Nova Science Publishers, New York, 2006), pp. 135–169.
[8] D. S. Grebenkov, Rev. Mod. Phys. **79**, 1077 (2007).
[9] R. Zwanzig, Proc. Natl. Acad. Sci. U. S. A. **87**, 5856 (1990).
[10] S. A. Allison, S. H. Northrup, and J. A. McCammon, J. Chem. Phys. **83**, 2894 (1985).
[11] G. Lamm and K. Schulten, J. Chem. Phys. **78**, 2713 (1983).
[12] S. J. Chapman, R. Erban, and S. A. Isaacson, SIAM J. Appl. Math. **76**, 368 (2016).
[13] R. Erban and S. J. Chapman, Phys. Biol. **4**, 16 (2007).
[14] J. Hattne, D. Fagne, and J. Elf, Bioinformatics **21**, 2923 (2005).
[15] K. R. Naqvi, K. J. Mork, and S. Waldenstrøm, Phys. Rev. Lett. **49**, 304 (1982).
[16] E. Jacob, Stochastic Proc. Appl. **122**, 191 (2012).
[17] M. A. El-Shehawey, J. Phys. A: Math. Gen. **33**, 9005 (2000).
[18] F. C. Goodrich, J. Chem. Phys. **22**, 588 (1954).
[19] D. S. Grebenkov, J. Phys. A: Math. Theor. **48**, 013001 (2014).
[20] J. S. Vrentas and C. M. Vrentas, Chem. Eng. Sci. **44**, 3001 (1989).
[21] I. P. Castillo and T. Dupic, J. Stat. Phys. **156**, 606 (2014).
[22] P. H. von Hippel and O. G. Berg, J. Biol. Chem. **264**, 675 (1989), and references therein.
[23] M. Slutsky and L. A. Mirny, Biophys. J. **87**, 4021 (2004); M. Coppey, O. Benichou, R. Voituriez, and M. Moreau, *ibid.* **87**, 1640 (2004); I. M. Sokolov, R. Metzler, K. Pant, and M. C. Williams, *ibid.* **89**, 895 (2005); Y. M. Wang, R. H. Austin, and E. C. Cox, Phys. Rev. Lett. **97**, 048302 (2006).
[24] D. S. Grebenkov, Phys. Rev. E **91**, 052108 (2015).
[25] R. Dickman and D. ben-Avraham, Phys. Rev. E **64**, 020102(R) (2001).
[26] A. V. Skorokhod, SIAM Theory Probab. Appl. **6**, 264 (1959); **7**, 3 (1959).
[27] K. Burdzy, Z. Q. Chen, and J. Sylvester, Ann. Probab. **32**, 775 (2004).
[28] A. Singer, Z. Schuss, A. Osipov, and D. Holcman, SIAM J. Appl. Math. **68**, 844 (2008).
[29] L. Batsilas, A. M. Berezhkovskii, and S. Y. Shvartsman, Biophys. J. **85**, 3659 (2003).
[30] A. M. Berezhkovskii, Y. A. Makhnovskii, M. I. Monine, V. Yu. Zitserman, and S. Y. Shvartsman, J. Chem. Phys. **121**, 11390 (2004).
[31] M. I. Monine and J. M. Haugh, J. Chem. Phys. **123**, 074908 (2005).
[32] M. A. Lomholt, I. M. Zaid, and R. Metzler, Phys. Rev. Lett. **98**, 200603 (2007).
[33] S. Stapf, R. Kimmich, and R. O. Seitter, Phys. Rev. Lett. **75**, 2855 (1995); P. Levitz *et al.*, *ibid.* **96**, 180601 (2006).
[34] B. Sapoval, Phys. Rev. Lett. **73**, 3314 (1994).
[35] A. A. Sonin, A. Bonfillon, and D. Langevin, Phys. Rev. Lett. **71**, 2342 (1993); C. Stenvot and D. Langevin, Langmuir **4**, 1179 (1988).
[36] E. R. Weibel, *The Pathway for Oxygen: Structure and Function in the Mammalian Respiratory System* (Harvard University Press, Cambridge, MA, 1984).
[37] B. Mauroy, M. Filoche, E. R. Weibel, and B. Sapoval, Nature (London) **427**, 633 (2004).
[38] B. Sapoval, M. Filoche, and E. R. Weibel, in *Branching in Nature*, edited by V. Fleury, J.-F. Gouyet, and M. Leonetti (EDP Sciences/Springer Verlag, Berlin, Heidelberg, 2001), pp. 225–242.
[39] B. Sapoval, J. S. Andrade Jr., and M. Filoche, Chem. Eng. Sci. **56**, 5011 (2001).
[40] J. S. Andrade Jr., M. Filoche, and B. Sapoval, Europhys. Lett. **55**, 573 (2001).
[41] J. S. Andrade Jr., H. F. da Silva, M. Baquil, and B. Sapoval, Phys. Rev. E **68**, 041608 (2003).
[42] A. J. Bray, S. N. Majumdar, and G. Schehr, Adv. Phys. **62**, 225 (2013).
[43] S. N. Majumdar, Curr. Sci. **89**, 2076 (2005).
[44] S. Redner, *A Guide to First-Passage Processes* (Cambridge University Press, Cambridge, MA, 2001).
[45] R. Metzler, G. Oshanin, S. Redner (eds.), *First-Passage Phenomena and Their Applications* (World Scientific, Singapore, 2014).
[46] O. Bénichou, C. Loverdo, M. Moreau, and R. Voituriez, Rev. Mod. Phys. **83**, 81 (2011).
[47] D. S. Grebenkov and J.-F. Rupprecht, J. Chem. Phys. **146**, 084106 (2017).
[48] P. Salminen and M. Yor, Period. Math. Hung. **62**, 75 (2011).

[49] E. Ben-Naim, S. Redner, and G. H. Weiss, J. Stat. Phys. **71**, 75 (1993).
[50] J. Whitehouse, M. R. Evans, and S. N. Majumdar, Phys. Rev. E **87**, 022118 (2013).
[51] H. Sano and M. Tachiya, J. Chem. Phys. **71**, 1276 (1979).
[52] K. D. Cole, J. V. Beck, A. Haji-Sheikh, and B. Litkouhi, *Heat Conduction Using Green's Functions* (CRC Press, Boca Raton, FL, 2010).
[53] P. L. Krapivsky, S. N. Majumdar, and A. Rosso, J. Phys. A: Math. Theor. **43**, 315001 (2010).
[54] S. Sabhapandit, S. N. Majumdar, and A. Comtet, Phys. Rev. E **73**, 051102 (2006).
[55] N. Agmon, J. Chem. Phys. **81**, 3644 (1984).
[56] A. M. Berezhkovskii, V. Zaloj, and N. Agmon, Phys. Rev. E **57**, 3937 (1998).
[57] B. T. Nguyen and D. S. Grebenkov, J. Stat. Phys. **141**, 532 (2010).
[58] D. S. Grebenkov, Phys. Rev. E **76**, 041139 (2007).
[59] M. D. Donsker and S. R. S. Varadhan, Commun. Pure Appl. Math. **28**, 1 (1975).
[60] A. C. Barato and R. Chetrite, J. Stat. Phys. **160**, 1154 (2015).
[61] S. S. Andrews, Phys. Biol. **6**, 046015 (2009).
[62] S. S. Andrews and D. Bray, Phys. Biol. **1**, 137 (2004).
[63] D. S. Grebenkov, R. Metzler, and G. Oshanin, New J. Phys. **19**, 103025 (2017).
[64] M. R. Evans and S. N. Majumdar, Phys. Rev. Lett. **106**, 160601 (2011).
[65] M. R. Evans and S. N. Majumdar, J. Phys. A: Math. Theor. **44**, 435001 (2011).
[66] A. Pal, Phys. Rev. E **91**, 012113 (2015).
[67] A. Pal and V. V. Prasad, Phys. Rev. E **99**, 032123 (2019).
[68] A. Pal and V. V. Prasad, Phys. Rev. Res. **1**, 032001(R) (2019).
[69] A. Pal, R. Chatterjee, S. Reuveni, and A. Kundu, J. Phys. A: Math. Theor. **52**, 264002 (2019).
[70] A. Pal, A. Kundu, and M. R. Evans, J. Phys. A: Math. Theor. **49**, 225001 (2016).
[71] A. Pal and S. Reuveni, Phys. Rev. Lett. **118**, 030603 (2017).

Correction: The affiliation listing for author I.P.C. required reformatting and has been fixed.